

## Determination of human absorbed dose from [ $^{153}\text{Sm}$ ]-Samarium maltolate based on distribution data in rats

H. Rezaeejam<sup>1</sup>, A. Hakimi<sup>2\*</sup>, A.R. Jalilian<sup>3</sup>, P. Abbasian<sup>2</sup>,  
S. Shirvani-Aran<sup>3</sup>, M. Ghannadi-Maragheh<sup>3</sup>

<sup>1</sup>Department of Medical Physics and Biomedical Engineering, Faculty of Medicine, Tehran University of Medical Sciences, Tehran, Iran

<sup>2</sup>Department of Energy Engineering and Physics, Amir Kabir University of Technology, Tehran, Iran

<sup>3</sup>Nuclear Science and Technology Research Institute, Tehran, Iran

### ABSTRACT

#### ► Original article

##### \* Corresponding author:

Mr. Amir Hakimi,

Fax: +98 21 22803280

E-mail: [amir.hakimi@aut.ac.ir](mailto:amir.hakimi@aut.ac.ir)

Revised: June 2014

Accepted: July 2014

Int. J. Radiat. Res., April 2015;  
13(2): 173-180

DOI: 10.7508/ijrr.2015.02.008

**Background:** Therapeutic radiopharmaceuticals are designed to deliver high doses of radiation to selected target organs with an aim of minimizing unwanted radiation to surrounding healthy tissue. Due to the potential of targeted radiotherapy to treat a wide range of malignant conditions, [ $^{153}\text{Sm}$ ]-samarium maltolate was developed for possible therapeutic applications. **Materials and Methods:** The organ radiation-absorbed doses have been evaluated for human based on animal data. After intravenous administration of  $^{153}\text{Sm}$ -Mal to four groups of rats, they were sacrificed at exact time intervals and the percentage of injected dose per gram of each organ was calculated by direct counting from rat data. Then S values for  $^{153}\text{Sm}$  by using specific absorbed fractions were calculated. By taking advantage of the formulation that Medical Internal Radiation Dose suggests, radiation-absorbed doses for all organs were calculated and extrapolated from rat to human. **Results:** From rat data, it is estimated that a 185-MBq injection of  $^{153}\text{Sm}$ -Mal into a human might result in the highest absorbed dose in the lymphoma tissues (liver 176.3, lungs 68, spleen 66.8 and sternum 19 mGy), especially in liver respect to the other tissues. **Conclusion:** These results suggest  $^{153}\text{Sm}$ -Mal as an efficiently new therapeutic agent in order to overcome possible lymphatic malignancies.

**Keywords:** Absorbed dose, biodistribution, MIRD, internal dosimetry,  $^{153}\text{Sm}$ -Mal.

### INTRODUCTION

Projecting radiotracer distribution and dosimetry across species from small animals such as rats to humans can be useful for accelerating the development of radioactive compounds to be used in clinical settings <sup>(1-2)</sup>.

Preclinical studies of radiopharmaceutical behavior are useful for predicting pharmacokinetics and metabolism in humans. Animal studies provide valuable distribution data for evaluating the potential utility of new

therapeutic radiopharmaceuticals <sup>(1)</sup>. Owing to the introduction of new therapeutic radiocompounds to deliver high doses of radiation to selected target organs with an aim of minimizing unwanted radiation to surrounding healthy tissue <sup>(5)</sup>, there is a need for efficient evaluation of the time-dependent distribution of such tracers in animals <sup>(2-4)</sup>.

Concerning to the recent project on the production and evaluation of lanthanide-based labeled compound using samarium-153 for targeted radionuclide therapy (TRT) applications <sup>(5-6)</sup>, the production of

[ $^{153}\text{Sm}$ ]-samarium maltolate was performed (7).

Radioisotopes with medium-energy beta emissions and half-life of a few days are attractive candidates for targeted irradiation (8). Samarium-153 has favorable radiation characteristics, medium-energy beta particle emissions ( $E_{\text{max}} = 808 \text{ keV}$ ) which is desirable for treatment, and range of about 3.0 mm in tissue has potential for targeted tumor radiotherapy (9). It emits medium-energy gamma photon (103 keV) in addition to particle emissions which make it suitable for monitoring the therapy with imaging, and for continuous follow-up of the absorbed dose distribution (5).

The use of targeted radionuclide therapy (TRT) for the treatment of cancer necessitates the development of dosing schedules that minimize the exposure of healthy tissues to radiation while maximizing the radiation dose received by the tumor (10). The aim in targeted radiotherapy is the selective delivery of radiation to cancer cells in a way that causes minimal toxicity to surrounding normal tissues. The basis for successful radionuclide therapy is selective concentration and prolonged retention of the radiopharmaceutical within the tumor (11). Maltol (3-Hydroxy-2-methyl-4-pyron) is commonly formed when sugars are heated. Maltol loses its hydroxyl proton at neutral to basic pH levels, forming the maltolate anion; this anionic molecule forms a strong bidentate/tridentate chelate with gallium, iron, zinc, aluminum, vanadium and many other metals (12). Most of maltolate metal complexes (e.g. Gallium-maltolate (13) and  $^{177}\text{Lu}$ -Maltolate (12)) are reported as biologically active compounds. Some of maltolate metal complexes are reported as biologically active compounds for lymphoma treatment (15) and apoptotic cell death (16).

Treatment with radiopharmaceuticals may result in abnormalities in other organs so it is important to estimate organ doses (17). Dosimetry represents meanwhile a precious guide for the selection of radionuclides as well as for therapy optimization (18). There exist various methods to estimate internal doses and new studies promises new perspective to come (19). Internal Commission on Radiological Protection (ICRP) and Medical Internal

Radiation Dose (MIRD) methodologies are the most commonly used internal dosimetry methods. The various ICRP and MIRD internal dosimetry models are similar in terms of their assumptions and defining equations. This similarity is obscured by differing terminology and notation, and these differences contribute to confusion in understanding these models (20).

The Committee on Medical Internal Radiation Dose of the Society of Nuclear Medicine developed a methodology to perform radiation absorbed dose calculations. These calculations are performed to assess the risks associated with the administration of radiopharmaceuticals for medical studies including imaging, therapy, and metabolic applications. The MIRD technique is a computational methodology that facilitates absorbed dose calculations to specified target organs from radioactive decays that occur in source organs. The source organs contain the radioactive material, and the target is the organ in which the dose is calculated. The target and source organs can be the same tissue. In subsequent discussion, the terms tissue and organ are used interchangeably. To specify the MIRD methodology, it is necessary to define several terms which detailed descriptions were presented in methods.

In this investigation, a precise description of organ distribution has been used owing to a large amount of distribution data (source organs in dosimetry calculations); efforts were taken to estimate the effective radiation dose absorbed into human organs following intra vascular administration of  $^{153}\text{Sm-Mal}$  by using the distribution data for normal rats.

## MATERIALS AND METHODS

Samarium-153 was produced by neutron irradiation of 1 mg of enriched [ $^{152}\text{Sm}$ ] $\text{Sm}_2\text{O}_3$  ( $^{152}\text{Sm}$ , 98.7% from ISOTECH Inc.) according to reported procedures (19) in the Tehran Research Reactor at thermal neutron flux of  $5 \times 10^{13} \text{ n cm}^{-2} \text{ s}^{-1}$  for 5d.  $^{153}\text{Sm}$  is produced according to the reaction  $^{152}\text{Sm} (n, \gamma) ^{153}\text{Sm}$  by  $\sigma = 206$  barns for thermal neutron and disintegrates via 3 main

routes by 100%  $\beta^-$  emission to levels in  $^{153}\text{Eu}$ .  $^{153}\text{Sm}$  is not a carrier free radioisotope and its specific activity was 22-28 GBq/mg. The irradiation  $^{153}\text{Sm}$  was dissolved in 200  $\mu\text{l}$  of 1.0 M HCl, to prepare  $^{153}\text{Sm}$  and diluted to the appropriate volume with ultra pure water, to produce a stock solution.

Chromatography paper (Whatman No. 2) was obtained from Whatman (Maidstone, UK). Radio-chromatography was performed using a Bioscan AR-2000 radio TLC scanner (Bioscan, Paris, France). A high purity germanium (HPGe) detector coupled with a Canberra™ (model GC1020-7500SL) multichannel analyzer and a dose calibrator ISOMED 1010 (Dresden, Germany) were used for counting distributed activities in rat organs. All other chemical reagents were purchased from Merck (Darmstadt, Germany). Calculations were based on the 103 keV peak for  $^{153}\text{Sm}$ . All values were expressed as mean  $\pm$  standard deviation (Mean $\pm$ SD) and the data were compared using Student's *t*-test. Statistical significance was defined as P value less than 0.05.

### Preparation of $^{153}\text{Sm-Mal}$

The labeling was developed in ethanolic media. Briefly,  $^{153}\text{SmCl}_3$  (111 MBq, 0.1 ml) was added to a borosilicate vial and dried by warming (50°C) under a nitrogen flow for about 15 minutes. Then, maltol (30mg, 0.25 mmol) dissolved in absolute ethanol (1 ml) was added to the dried residue and the mixture agitated and incubated at 60°C for 2 hours. The radiochemical purity<sup>(21)</sup> of free samarium and Sm-MAL were determined by counting Whatman No.2 sheets as stationary phase using various mobile phases (A: ammonia:water:methanol (2:40:20), B: 1mM DTPA aqueous solution, C: %10 ammonium acetate:methanol system, 1:1). After obtaining the desired radiochemical purity, the ethanolic solution was concentrated by warming 40–50°C to 0.05 ml and then diluted to a 5% solution by adding 1 ml of normal saline.

### Biodistribution studies of radiopharmaceutical

The distribution of  $^{153}\text{Sm-Mal}$  among tissues was determined for untreated rats. Five male

rats each were sacrificed by  $\text{CO}_2$  asphyxiation (after anesthesia induction using propofol/xylazine mixture) at 2, 4, 24, 28 and 96 h (3 rats in each time) after injection of  $4.80 \pm 0.18$  MBq of final complex through their tail vein and exsanguinated, and the tissues (blood, heart, lung, spleen, intestine, kidneys, liver, muscle and bone) were rapidly removed. During the entire study, autoclaved food and drinking water were available *ad libitum*. Animal studies were carried out in accordance with the UK Biological Council's Guidelines of the Use of Living Animals in Scientific Investigations, 2<sup>nd</sup> edition<sup>(22)</sup> (approved by Iranian Ministry of Health and Medical Education).

### Activity measurement

The activity in the syringes was measured before the injection and then after administration of the radiopharmaceutical products with the well-type ionization chamber (CRC-15R, Capintec, Ramsey, New Jersey, USA), all measurements were background subtracted and then averaged together. Uncertainties in the determinations were minimal, because each assay collected at least 1000 count.

For each of these measurements, three samples were weighed and then counted by HPGe detector to determine the percentage of injected activity per gram (%IA/g) (which was equivalent to the percentage of injected activity per gram %IA/gr  $\equiv$  Percentage injected dose per gram %ID/gr); all the organ activity measurements were normalized to injected activity. All samples were background-subtracted and nondecay-corrected to the time of killing, and then similar samples were averaged together.

To convert the counts to activity, following formula was used:

$$\text{Activity (Bq)} = \frac{\text{Area}}{t \times \text{Eff} \times Br} \quad (1)$$

Where the "area" term is the number of counts in the selected window (in the confined energy) and the *t* represents the counting time in this study; it was 100s and the term "Eff" is the detector efficiency (in the selected energy) were given from the detector manual and the term

"Br" is defined as the decay yield of the selected gamma energy.

The  $^{153}\text{Sm}$  activity concentration at time  $t$ ,  $C_{\text{tissue}}(t)$  was then calculated the percentage of injected activity per gram of tissue (%IA/g) with equation (2):

$$C_{\text{tissue}} = \frac{A_{\text{tissue}}(t) / M_{\text{tissue}}}{A_{\text{total}}} \times 100 \quad (2)$$

Where  $A_{\text{tissue}}(t)$  is the  $^{153}\text{Sm}$  activity in the sample,  $M_{\text{tissue}}$  is the mass of the sample and  $A_{\text{total}}$  is the total activity of  $^{153}\text{Sm}$  injected into the rat.

### Estimate the human absorbed dose from rat data

To extrapolate biokinetic data from animals to humans different methods have been previously used <sup>(23)</sup>. The proposed method of Sparks and Aydogan <sup>(24)</sup> on the basis of percent injected dose (or injected activity) per gram (%ID/gr) unit was used as follows:

$$\%ID_{\text{HumanOrgan}} = \%ID_{\text{AnimalOrgan}} \frac{\frac{\text{OrganMass}_{\text{human}}}{\text{BodyMass}_{\text{human}}}}{\frac{\text{OrganMass}_{\text{animal}}}{\text{BodyMass}_{\text{animal}}}} \quad (3)$$

The mean weight of the organs harvested from the animals and standard weights established for the adult male human organs <sup>(25-27)</sup> was used. The rat's organ masses and the ration of organ mass to body mass in humans and in rats are shown in table 1 according to peters and Boyd <sup>(28)</sup>.

**Table 1.** The rat's organ masses and the ratio of organ mass to body mass in human and in rat.

Tissues	Rat (%)	Weight (g)	Human <sup>a</sup> (%)
Adrenal	0.03	0.04	0.02
Urine	0.06	0.09	0.52
Intestine	0.60	0.90	0.22
Kidney	0.78	1.17	0.44
Liver	4.28	6.42	2.57
Lung	0.66	0.98	1.42
Muscle	53.4	80.16	68.6
Ovary	0.03	0.04	0.02
Pancreas	0.31	0.47	0.14
Bone	1.00	1.5	1.43
Skin	19.9	29.9	13.0
Spleen	0.36	0.54	0.53

<sup>a</sup> Human data according to ICRP 22 <sup>(23)</sup>.

### Dosimetric calculations

For each group of rats, the non-decay corrected time activity curves were generated for the source organs including the followings: the lung, kidney, spleen, liver, a trabecular bone and blood.

The distribution data were plotted out, and the points were fitted to a single exponential equation by the least-squares linear regression method from radioactivity from individual organs, fitted a mono-exponential curve.

The non-decay-corrected time-activity curves were extrapolated to infinity by fitting the tail of each curve to a mono-exponential and integrated, resulting in a concentration integral for each organ. The data points representing the percentage-injected dose (%ID/organ) were created and fitted to a mono-exponential, a bi-exponential or an uptake-and-clearance curve. The rat data were assumed to approximate the biokinetic parameters in the human.

The use of tables presented in the Medical Internal Radiation Dose (MIRD) No. 11 <sup>(29)</sup> which are used to compute the absorbed dose, it is necessary to calculate the cumulated source activity ( $A_h$ ) in each organ according to the equation (4):

$$\tilde{A}_h = \int_{t1}^{\infty} A_h(t) dt \quad (4)$$

The liver, kidneys, blood, spleen, lung, stomach, Lower large Intestine, colon, muscle, heart, sternum and trabecular bone were used as the primary source organs. The MIRD formulation was applied to calculate the absorbed radiation dose for various organs <sup>(30)</sup>.

$$\tilde{D}_{(rk)} = \sum_h \tilde{A}_h S(r_k \leftarrow r_h) \quad (5)$$

Where the mean absorbed dose  $\tilde{D}_{(rk)}$  stated in (mGy) to a target organ  $r_k$  from a radiopharmaceutical distributed identically in a source organ  $r_h$  has been formulated by the MIRD committee. The  $S(r_k \leftarrow r_h)$  expressed in (mGy/MBq<sup>s</sup>) represented the specific absorbed fraction of energy for the target organ  $r_k$  for particles emitted in the source organ  $r_h$  <sup>(31)</sup>.



**Radiation-absorbed dose calculation**

Methods compatibles with those recommended by the MIRD Committee of the Society of Nuclear Medicine were used to determine the absorbed doses to the human normal organs and the whole body <sup>(32-33)</sup>.

**RESULTS**

Table 2 demonstrated the accumulation of <sup>153</sup>Sm-Mal in the major organs. In addition the clearance curves from each organ of the rats shown in figure 1. The results showed that most of the activity was accumulated in the liver. The absorption of the colon, Lower large Intestine, muscle and stomach was absolutely negligible, and it was very interesting because the samarium-153 chelates e.g. <sup>153</sup>Sm-EDTMP, <sup>153</sup>Sm-NTMP, <sup>153</sup>Sm-HEEDTMP, <sup>153</sup>Sm-NBTP and <sup>153</sup>Sm-NTA major absorption were in the skeletal system <sup>(34)</sup>, but in complex <sup>153</sup>Sm-Mal the major absorption was in the liver. It means that the absorption of new complex is completely different from other samarium-153 chelates that are potential therapeutic bone agents.

The radiation absorbed organ doses estimated in humans according to the biological data from the rat study are shown in table 3.

**Table 3.** The Human absorbed dose estimation.

Organs	Absorbed dose (mGy/MBq) <sup>a</sup>	Absorbed dose (mGy) <sup>b</sup>
Adrenals	0.0164	3.0340
Bladder wall	0.00696	1.2876
Bone	0.119	22.015
Brain	0.00723	1.3375
Breasts	0.00816	1.5096
Stomach wall	0.01003	1.8555
Heart wall	0.0220	4.070
Kidneys	0.244	45.140
Liver	0.953	176.305
Lungs	0.368	68.080
Ovaries	0.00779	1.4411
Pancreas	0.0153	2.8305
Red marrow	0.0996	18.426
Skin	0.00711	1.3153
Spleen	0.361	66.785
Testes	0.00669	1.2376
Thyroid	0.00721	1.3338
Uterus	0.00784	1.4504
Total body	0.3483	64.4355

<sup>a</sup> Might had some over/under estimation according to table 3.

<sup>b</sup> 185 MBq Injected Activity

The rats' biodistribution data were projected into the humans. A 185-MBq (5-mCi) injection of <sup>153</sup>Sm-Mal into the human body might result in an estimated absorbed dose of 53.22 mGy for the total body and the highest absorbed dose was observed in the liver with 151.14 mGy followed by spleen, lungs, kidneys, bone and red marrow tissues received 64.01, 52.35, 34.04, 18.87 and 18.13 mGy respectively.

**Table 2.** Distribution of <sup>153</sup>Sm-Mal in different time points.

Organs	Time (Mean <sup>a</sup> ±SD)				
	2 h	4 h	24 h	48 h	96h
Blood	1.0969 ± 0.125	0.8861 ± 0.11	0.1543 ± 0.03	0.0607 ± 0.02	0.008 ± 0.001
Heart	0.6494 ± 0.16	0.0694 ± 0.01	0.1351 ± 0.04	0.2426 ± 0.06	0.1163 ± 0.04
Lung	0.5423 ± 0.11	0.5717 ± 0.10	0.2018 ± 0.06	0.0980 ± 0.03	0.0433 ± 0.007
Stomach	0.0874 ± 0.01	0.1846 ± 0.02	0.0754 ± 0.00	0.0175 ± 0.00	0.0019 ± 0.000
Colon	0.0335 ± 0.00	0.1152 ± 0.02	0.0273 ± 0.00	0.0249 ± 0.00	0.0103 ± 0.00
Intestine	0.1446 ± 0.02	0.1599 ± 0.03	0.0517 ± 0.01	0.0042 ± 0.00	0.0004 ± 0.000
Liver	4.6164 ± 0.4	6.1051 ± 0.35	3.2293 ± 0.37	0.8590 ± 0.13	0.2439 ± 0.08
Spleen	1.0166 ± 0.3	1.3231 ± 0.16	1.5545 ± 0.47	0.1482 ± 0.06	0.023 ± 0.003
Kidney	0.8232 ± 0.12	0.7729 ± 0.31	0.7591 ± 0.16	0.5676 ± 0.09	0.012 ± 0.004
Muscle	0.0753 ± 0.02	0.0261 ± 0.00	0.0842 ± 0.00	0.0446 ± 0.01	0.01962 ± 0.02
Sternum	0.1938 ± 0.04	0.2968 ± 0.03	0.1601 ± 0.02	0.6909 ± 0.08	0.304 ± 0.064
Thigh Bone	0.4438 ± 0.06	0.5590 ± 0.10	0.7005 ± 0.08	0.0896 ± 0.02	0.0012 ± 0.000

<sup>a</sup> Data were presented as the percentage of administrated activity per gram (non-decay corrected).

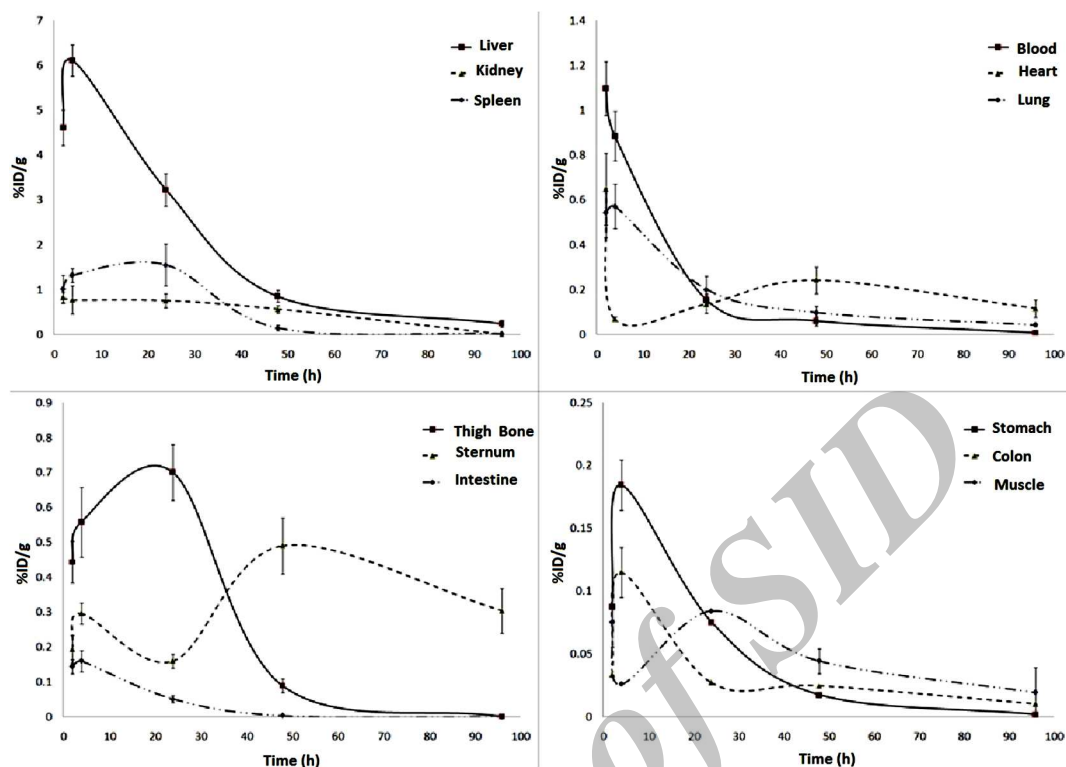


Figure 1. The clearance curves from each organ of the rats.

## DISCUSSION

In rat studies, the tracer was mostly accumulated in the liver, which was the major organ of accumulation throughout the study as shown in table 2. The liver to blood activity concentration ratio was about 20 at 24 h and up to 14 at 48 h post-injection. The livers to muscle ratios were more than 30 at 24 and about 20 at 48 h post-injection.

There are four methods using animal data to predict human residence times: first, no extrapolation assumes that the percentage of injected activity ( $\%IA \equiv \%ID$ ) at any time in the human organ is the same as in the animal organ. Second, relative organ mass extrapolation study was carried out, third using physiological time extrapolation and fourth, using a combination of the mass and time methods by applying both the mass and physiological time extrapolations to the animal data <sup>(24)</sup>.

The amount of the radiation-absorbed dose to a human was calculated by determining the distributions in rats, obtaining a cumulated

activity value, multiplying by the ratio of organs to extrapolate to humans (using relative organ mass extrapolation) and then multiplying the converted rats' cumulative activity to the S factor table of  $^{153}\text{Sm}$  <sup>(35-36)</sup>. For humans, the highest radiation-absorbed doses per unit-administered activity were calculated for liver (0.953 mGy/MBq), lungs (0.361 mGy/MBq) and spleen (0.368 mGy/MBq). The absorbed doses to the kidneys, bone and red marrow were less than 0.2 mGy per MBq. The total body dose was estimated to be 0.348 mGy/MBq as shown in table 3. The discrepancy between different animal models is important if absorbed dose estimations for humans are derived from animal models. Obviously the distribution of a radiopharmaceutical parameter varies not only from rodents to humans, but also between rats and mice <sup>(37-39)</sup>.

Extrapolation between various animal species is more reliable than extrapolation between animals and humans <sup>(24)</sup>, but previous studies have demonstrated the usefulness of using animal distribution as a model for absorbed dose estimations in humans <sup>(40-43)</sup>.

Using physiological time extrapolation improves the mean result. However, there appears to be some increase in severe overestimates (more than 10-fold) with the time extrapolation method <sup>(24)</sup>. Using the physiological time extrapolation is not valid for this study because one cannot estimate the exact value resident time. Therefore, for this study using relative organ mass extrapolation is more precise than physiological time extrapolation.

New therapeutic radiopharmaceutical significantly accumulated in liver and increased after administration for 4 h. Blood and heart uptake showed their maximum at first 2 h and then decreased as shown in figure 1.

## CONCLUSION

Radiation dosimetry for  $^{153}\text{Sm-Mal}$  was estimated for humans based on distribution data of  $^{153}\text{Sm-Mal}$  in normal rats. The distribution of  $^{153}\text{Sm-Mal}$  in rats demonstrated significant liver uptake and low muscle and blood uptake; however, the kidney uptake is somewhat high. The hypothesis for high uptake of the kidney is excretion of the complex by the urinary system 2 h post-injection till 48 h post-injection.

Although further dosimetry work should be performed on humans as this compound become useful in the clinic, these estimates can be used to predict potential absorbed doses in humans and for planning human studies.

**Conflicts of interest:** none to declare.

## REFERENCES

- Shanehsazzadeh S, Jalilian AR, Sadeghi HR, Allahverdi M (2009) Determination of human absorbed dose of 67GA-DTPA-ACTH based on distribution data in rats. *Radiation protection dosimetry*, **134**(2): 79-86.
- Moghaddam AK, Jalilian AR, Hayati V, Shanehsazzadeh S (2010) Determination of human absorbed dose of 201Tl (III)-DTPA-HlgG based on biodistribution data in rats. *Radiation protection dosimetry*, **141**(3): 269-274.
- Abbasian P, Foroghy M, Jalilian AR, Hakimi A Shirvani-Arani S (2014) Modeling the time dependent biodistribution of Samarium-153 ethylenediamine tetramethylene phosphonate using compartmental analysis. *Reports of Practical Oncology & Radiotherapy*, **19**(3): 214-220.
- Sardari D and Hakimi A (2012) Modeling the time dependent distribution of a new  $^{153}\text{Sm}$  complex for targeted radiotherapy purpose. *Reports of Practical Oncology and Radiotherapy*, **17**(6): 358-362.
- Naseri Z, Hakimi A, Shirvani-Arani S, Jalilian AR, Bahrami-Samani A, Nemati Kharat M, Ghannadi-Maragheh M (2012) Preparation and quality control of  $^{153}\text{Sm}$ -[tris (1, 10-phenanthroline) samarium (III)] complex. *Int J Radiat Res*, **10**(1): 59-62.
- Naseri Z, Hakimi A, Jalilian AR, Nemati Kharat A, Shirvani-Arani S, Bahrami-Samani, Ghannadi-Maragheh M (2012) Synthesis, quality control and biological evaluation of tris [(1, 10-phenanthroline)[ $^{153}\text{Sm}$ ] samarium (III)] trithiocyanate complex as a therapeutic agent. *Radiochimica Acta*, **100**(4): 267-271.
- Naseri Z, Hakimi A, Jalilian AR, Kharat AN, Bahrami-Samani A, Ghannadi-Maragheh M (2011) Preparation and quality control of the [ $^{153}\text{Sm}$ ]-samarium Maltolate Complex as a Lanthanide Mobilization Product in Rats. *Scientia pharmaceutica*, **79**(2): 265.
- Anderson PM, Wiseman GA, Dispenzieri A, Arndt CA, Hartmann LC, Smithson WA, Bruland OS (2002) High-dose samarium-153 ethylene diamine tetramethylene phosphonate: low toxicity of skeletal irradiation in patients with osteosarcoma and bone metastases. *Journal of Clinical Oncology*, **20**(1): 189-196.
- Hakimi A, Jalilian AR, Arani SS, Samani AB, Maragheh MG, Arbabi A (2010) Preparation and quality control of  $^{153}\text{Sm}$ -[tris (1, 10-phenanthroline) samarium (III)] complex as a therapeutic compound. *Iranian Journal of Nuclear Medicine*, **18**(Suppl 1): 111.
- Ferl GZ, Kenanova V, Wu AM, DiStefano JJ (2006) A two-tiered physiologically based model for dually labeled single-chain Fv-Fc antibody fragments. *Molecular cancer therapeutics*, **5**(6): 1550-1558.
- Ersahin D, Doddamani I, Cheng D (2011) Targeted radionuclide therapy. *Cancers*, **3**(4): 3838-3855.
- Bernstein LR, Tanner T, Godfrey C, Noll B (2000) Chemistry and pharmacokinetics of gallium maltolate, a compound with high oral gallium bioavailability. *Metal Based Drugs*, **7**: 33-48.
- Chitambar CR, Purpi DP, Woodliff J, Yang M, Wereley JP (2007) Development of gallium compounds for treatment of lymphoma: gallium maltolate, a novel hydroxypyrrone gallium compound, induces apoptosis and circumvents lymphoma cell resistance to gallium nitrate. *Journal of Pharmacology and Experimental Therapeutics*, **322**(3): 1228-1236.
- Hakimi A, Jalilian AR, Arani SS, Samani AB, Maragheh MG, Arbabi A (2010) Production and evaluation of Lutetium-177 Maltolate as a possible therapeutic agent. *Iranian Journal of Nuclear Medicine*, **18**(Suppl 1): 143.
- Thompson KH, Barta CA, Orvig C (2006) Metal complexes of maltol and close analogues in medicinal inorganic chemistry. *Chemical Society Reviews*, **35**(6): 545-556.
- Eiko S, Iho Y, Yamada T, Suzuki Y, Ohyashiki T (2007)

- Involvement of NO generation in aluminum-induced cell death. *Biological and Pharmaceutical Bulletin* 30, no. 8: 1390-1394.
17. Shahbazi-Gahrouei D and Nikzad S (2011) Determination of organ doses in radioiodine therapy using medical internal radiation dosimetry (MIRD) method. *Int J Radiat Res*, **8(4)**: 249-252.
  18. Schuchardt C, Kulkarni HR, Prasad V, Zachert C, Müller D, Baum RP (2013) The Bad Berka dose protocol: Comparative results of dosimetry in peptide receptor radionuclide therapy using  $^{177}\text{Lu}$ -DOTATATE,  $^{177}\text{Lu}$ -DOTANOC, and  $^{177}\text{Lu}$ -DOTATOC. In *Theranostics, Gallium-68, and Other Radionuclides* (pp. 519-536). Springer Berlin Heidelberg.
  19. Cremonesi M, Ferrari M, Di Dia A, Botta F, De Cicco C, Bodei L, Paganelli G (2011) Recent issues on dosimetry and radiobiology for peptide receptor radionuclide therapy. *Journal of Nuclear Medicine and Molecular Imaging*, **55(2)**: 155-167.
  20. Bevelacqua JJ (2005) Internal dosimetry primer. *Radiation Protection Management*, **22(5)**: 7.
  21. Jalilian AR, Hakim A, Garousi J, Bolourinovin F, Kamali-Dehghan M, Aslani G (2008) Development of  $^{201}\text{Tl}$ (III) oxinate complex for *in-vitro* cell labeling. *Int J Radiat Res*, **6(3)**: 145-150.
  22. Manual for produced radioisotopes, IAEA, Vienna (2003) IAEA-TECDOC-1340, ISBN 92-0-101103-2, ISSN 1011-4289, © IAEA (2003), P. 71, printed by the IAEA in Austria, January 2003.
  23. ICRP, (1992) Radiological Protection in Biomedical Research. ICRP Publication 62. Ann. ICRP 22 (3).
  24. Sparks RB and Aydogan B (1999) Comparison of the effectiveness of some common animal data scaling techniques in estimating human radiation dose. In *Sixth International Radiopharmaceutical Dosimetry Symposium*. Stelson AS, editor. Oak Ridge: Associated Universities (pp. 705-716).
  25. Richmond CR (1986) ICRP publication 23. *International Journal of Radiation Oncology\* Biology\* Physics*, **12(3)**: 433.
  26. Loevinger R, Budinger TF, Watson EE (1988) MIRD primer for absorbed dose calculations. New York: Society of Nuclear Medicine.
  27. Cristy M and Eckerman KF (1987) Specific Absorbed Fractions of Energy at Various Ages from Internal Photon Sources: 1, Methods. Atomic Energy Research Establishment.
  28. Peters JM and Boyd EM (1966) Organ weights and water levels of the rat following reduced food intake. *The Journal of Nutrition*, **90(4)**: 354-360.
  29. Snyder WS, Ford MR, Warner GG, Watson SB (1975) S" absorbed dose per unit cumulated activity for selected radionuclides and organs. MIRD Pamphlet No. 11. *Society of Nuclear Medicine*, New York.
  30. Snyder WS, Ford MR, Warner GG (1978) MIRD pamphlet no. 5, revised: Estimates of specific absorbed fractions for photon sources uniformly distributed in various organs of a heterogeneous phantom. New York, NY: Society of Nuclear Medicine.
  31. ICRU, Methods of assessment of absorbed dose in clinical use of radionuclides. Report No. 32 (Washington, DC: ICRU) (1979).
  32. Benedetto AR (1986) NCRP Report No. 83, The Experimental Basis for Absorbed-Dose Calculations in Medical Uses of Radionuclides National Council on Radiation Protection and Measurements, Bethesda, NCRP Publications, 1985. *Journal of Nuclear Medicine*, **27(8)**: 1378-1379.
  33. Goeckeler WF, Edwards B, Volkert WA, Holmes RA, Simon J, Wilson D (1987) Skeletal localization of samarium-153 chelates: potential therapeutic bone agents. *Journal of Nuclear Medicine*, **28(4)**: 495-504.
  34. Goeckeler WF, Edwards B, Volkert WA, Holmes RA, Simon J, Wilson D (1987) Skeletal localization of samarium-153 chelates: potential therapeutic bone agents. *Journal Nuclear Medicine*, **28(4)**: 495-504.
  35. Radfar E, Jalilian AR, Yousefnia H, Bahrami-Samani A, Ghannadi-Maragheh M (2012) A comparative study of preliminary dosimetry for human based on distribution data in rats with  $^{111}\text{In}$ ,  $^{90}\text{Y}$ ,  $^{153}\text{Sm}$ , and  $^{177}\text{Lu}$  labeled rituximab. *Nuclear Technology and Radiation Protection*, **27(2)**: 144-151.
  36. Logan KW, Volkert WA, Holmes RA (1987) Radiation dose calculations in persons receiving injection of samarium-153 EDTMP. *J Nucl Med*, **28**: 505-509.
  37. Schmitt A, Bernhardt P, Nilsson O, Ahlman H, Kölbly L, Maecke HR, Forsell-Aronsson E (2004) Radiation therapy of small cell lung cancer with  $^{177}\text{Lu}$ -DOTA-Tyr3-octreotate in an animal model. *Journal of Nuclear Medicine*, **45(9)**: 1542-1548.
  38. de Jong M, Breeman WA, Bernard BF, Bakker WH, Schaar M, van Gameren A, et al. (2001) [ $^{177}\text{Lu}$ -DOTA0, Tyr3] octreotate for somatostatin receptor-targeted radionuclide therapy. *International Journal of Cancer*, **92(5)**: 628-633.
  39. Lewis JS, Wang M, Laforest R, Wang F, Erion JL, Bugaj JE, Anderson CJ (2001) Toxicity and dosimetry of  $^{177}\text{Lu}$ -DOTA-Y3-octreotate in a rat model. *International Journal of Cancer*, **94(6)**: 873-877.
  40. Palm S, Enmon RM, Matei C, Kolbert KS, Xu S, Zanzonico PB, Sgouros G (2003) Pharmacokinetics and biodistribution of  $^{86}\text{Y}$ -trastuzumab for  $^{90}\text{Y}$  dosimetry in an ovarian carcinoma model: correlative MicroPET and MRI. *Journal of Nuclear Medicine*, **44(7)**: 1148-1155.
  41. Deterding TA, Votaw JR, Wang CK, Eshima D, Eshima L, Keil R, et al. (2001) Biodistribution and radiation dosimetry of the dopamine transporter ligand [ $^{18}\text{F}$ ] FECNT. *Journal of Nuclear Medicine*, **42(2)**: 376-381.
  42. Bélanger MJ, Krause SM, Ryan C, Sanabria-Bohorquez S, Li W, Hamill TG, Burns HD (2008) Biodistribution and radiation dosimetry of [ $^{18}\text{F}$ ] F-PEB in nonhuman primates. *Nuclear Medicine Communications*, **29(10)**: 915-919.
  43. Kesner AL, Hsueh WA, Czernin J, Padgett H, Phelps ME, Silverman DH (2008) Radiation dose estimates for [ $^{18}\text{F}$ ] 5-Fluorouracil derived from PET-based and tissue-based methods in rats. *Molecular Imaging and Biology*, **10(6)**: 341-348.